DETECTION OF CURBSTONES IN AIRBORNE LASER SCANNING DATA

George Vosselman [a], Zhou Liang [b]

[a] International Institute for Geo-Information Science and Earth Observation (ITC), Enschede, the Netherlands
vosselman@itc.nl,
[b] Heilongjiang Bureau of Surveying and Mapping, Harbin, China
zhou19153@itc.nl

Commission III, WG III/2

KEY WORDS: feature extraction, road detection, airborne laser scanning

ABSTRACT:

The high point densities obtained by today's airborne laser scanners enable the extraction of various features that are traditionally mapped by photogrammetry or land surveying. While significant progress has been made in the extraction of buildings and trees from dense point clouds, little research has been performed on the extraction of roads. In this paper it is analysed to what extent road sides can be mapped in point clouds of high point density (20 pts/m^2). In urban areas curbstones often separate the road surface from the adjacent pavement. These curbstones are mapped in a three step procedure. First, the locations with small height jumps near the terrain surface are detected. Second, midpoints of high and low points on either side of the height jump are generated, put in a sequence, and used to fit a smooth curve. Third, small gaps between nearby and collinear line segments are closed. GPS measurements were taken to analyse the performance of the road side detection. The analysis showed that the completeness varied between 50 and 86%, depending on the amount of parked cars occluding the curbstones. The RMSE in the comparison with the GPS measurements was 0.18 m.

1. INTRODUCTION

With the high pulse rates of the current laser scanners, point densities of 10-20 pts/m^2 can easily be obtained from low flying platforms. These point densities enable the use of laser scanning data for various mapping tasks, like the extraction of building outlines (Clode et al., 2004a; Wang et al., 2006; Sampath and Shan, 2007), change detection (Matikainen et al., 2003; Vosselman et al., 2005), 3D building modelling (Brenner, 2005; Rottensteiner, 2003), and the detection of single trees (Hyyppä and Inkinen, 1999; Persson et al., 2002).

So far, less research focussed on the extraction of road geometries. Clearly, height differences are less prominent and often also less relevant for mapping roads. Clode et al. (2004b) used the pulse reflectance strength and a DTM to detect roads in a point cloud with a density of 1 pt/m^2. Later, they improved the detection by using areas already classified as building or vegetation as constraint. After thinning and vectorisation, road centrelines were obtained. Akel et al. (2005) detected road areas by classifying smooth segments based on size and shape characteristics. Rieger et al. (1999) used the surface slope in a 20 cm elevation grid to detect roads in mountainous areas. Hatger and Brenner (2003, 2005) used laser scanning data with a point spacing of 0.5 m to extract properties of roads for which the centrelines are known from a road database. Properties may include height, longitudinal and transversal slope, curvature, and width. Height profiles across the road are split into to straight segments. A RANSAC procedure on the end points of the segments with low slope values is used to fit straight lines to the road sides.

In this paper a method is presented which delineates curved and straight road sides without the usage of known road centrelines. The method is based on the detection of small height jumps in the data caused by curbstones separating the road surface from the pavement. Curbstones of only 10 cm height can be clearly seen in data acquired by airborne laser scanners. Fig. 1 shows a curbstone in a dataset with 20 pts/m^2 as recorded by the FLI-MAP 400 laser scanner (Fugro Aerial Mapping, 2009). Fitting a planar surface to either side of the curbstone results in an estimated height standard deviation of 1-2 cm. As all points within a small neighbourhood are based on the same GPS/IMU observations, the shape of the road edges is not affected by noise in these observations. The dispersion seen in Fig. 1 is only caused by the noise in the measurements of the laser range finder. These instruments are indeed known to be accurate to 1-2 cm. Hence, the signal-to-noise ratio is very favourable for the detection of curbstones.

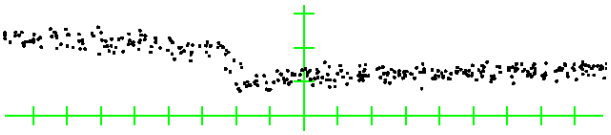

Fig. 1: Points on a profile across a road side with a curbstone. The tick spacing is 10 cm.

The next section elaborates on the method developed for the detection of road sides in high resolution airborne laser scanning data. Results on three road junctions are presented and analysed in section 3. The completeness of the detected road sides is evaluated by a comparison with road sides manually delineated in an orthophoto. The accuracy is analysed by comparing the extracted road sides to GPS measurements.

2. CURBSTONE DETECTION METHOD

The developed curbstone detection method consists of three steps. First, the locations with small height jumps near the terrain surface are detected. These are potential locations of curbstones. Second, midpoints of high and low points on either side of the height jump are generated. These are put in sequence and are used to fit a smooth curve. Finally, small gaps between nearby and collinear line segments are closed.

2.1 Detection of locations with small height jumps

To decide whether a point could be near the road side, a neighbourhood was defined for each point and the height distribution of the points within the neighbourhood was analysed. In the used dataset points where considered neighbouring if the planimetric distance between the points was less than 50 cm. For each point neighbourhood, the following three criteria were evaluated.

a) The maximum height difference within the neighbourhood should be below the maximum expected height of a curbstone plus some tolerance for the noise in the range measurement. This criterion excludes areas with large height variations due to buildings, trees, cars, or other objects.
b) The height variation within the neighbourhood should be larger than the variation caused by the range measurement noise. In the used dataset a standard deviation of 3-4 cm already indicated the presence of a height signal.
c) The points in the neighbourhood should be close to the terrain surface. For the used dataset a DTM was derived by a segment based filtering approach. This criterion excluded neighbourhoods with small height differences that may be found on roofs.

In some areas of the dataset it was found that the thresholding on the height standard deviation (criterion b) led to many detected potential road sides in the middle of the road surface. A closer inspection of the data revealed that these areas contained data from two different strips (Fig. 2). The height difference of 5 cm between the strips caused a significant increase in the calculated standard deviation. To avoid this problem, the detection of locations with small height jumps was performed on a strip by strip basis.

Fig. 2: Systematic height differences between data of two strips.

An example of points with neighbourhoods fulfilling the three criteria listed above is shown in Fig. 3(a). The selected points are on either side of the small jump edge. To obtain an estimation of the jump edge location, the points are classified as points belonging to the higher and lower surface. For each point on the higher surface the nearest point on the lower surface is computed. Vice versa, the nearest point on the higher surface is computed for each point on the lower surface. Pairs of points from the higher and lower surface are then selected for which both points are each other's nearest point on the other surface. For these point pairs the midpoints are taken as an estimation of the jump edge location. With this procedure it is assured that midpoints are only taken between points that are relatively nearby. Without using any further information on the distribution of the points, the midpoint is the location with the smallest expected error in the location of the height jump. Fig. 3(b) shows the derived mid points of the selected points in Fig. 3(a).

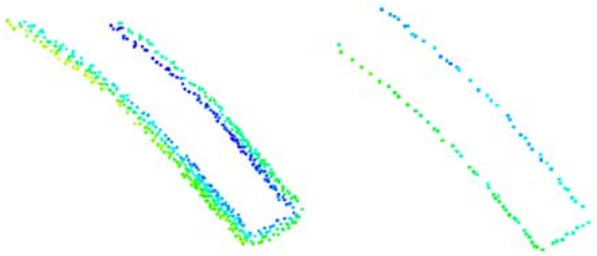

(a) (b)

Fig. 3: Selected points around a small height jump (a). Derived midpoints as approximation for the height jump location (b).

2.2 Reconstructing the line topology

Although the determined midpoints visually already form a smooth description of the road sides, the result obtained so far is just a set of points and does not contain any topological information. Within the processed area there will most often be various (pieces of) road sides with small height jumps. To collect the points that belong to the same road side piece, a connect component labelling is performed on the midpoints. All points that can be connected to each other through small steps from point to point are given the same label (Fig. 4).

Fig. 4: Connected components of nearby midpoints

Each connected component is then processed separately. Components with only a small number of points are ignored as they are most likely the result of some low vegetation. For the other components RANSAC (Fischler and Bolles, 1981) is used to find a set of points that are on a (nearly) straight line. Sorted along the line, these points constitute the initial road side polygon that is then extended with further points of the component. At both sides of this polygon points are added if they are within some distance of the polygon end. Preference is given to points for which the vector between the polygon end and the point has the smallest angle with the last edge of the polygon. This search continues until no further nearby points are found or until the polygon is closed.

2.3 Bridging gaps in road side outlines

In the results of the previous step one will often see gaps in the detected road sides. These gaps are usually caused by parked cars that are occluding the road side or by the absence of curbstones (and height jumps) at carriage drives or at road crossing locations for wheel chairs. In order to complete the

road side descriptions as far as possible, rules were defined for closing small gaps between detected road side segments.

a) Two straight line segments that are collinear are connected if no other line segment is present in the gap between them. The same rule is also applied to line segments for which the last five points on either side are on a straight line.
b) Pairs of line segments left after the application of the above rule are also connected if the distance between the extension of one loose end and the end point of the other segment is below some threshold.

In both cases, only gaps of a certain maximum size will be closed. Line segments with a limited length after the completion of the gap bridging procedure were removed. The various required thresholds were optimised by trial and error.

Finally, B-splines are fit with the de Boor-Cox algorithm to generate smooth curves for the road sides (de Boor, 1978). Further details on the algorithm for road side extraction can be found in (Zhou, 2009).

3. RESULTS AND ANALYSIS

Three road crossings from a dataset with 20 pts/m^2 were processed with the method described in the previous section. The first road crossing is a larger one with an elevated bus lane, some separated cycle lanes and many traffic islands. The other two crossings are located in a residential area. The results are visualised using two figures for each crossing. The Figs. 5-10 all use colour coded heights. In Figs. 5, 7 and 9 the full colour range is re-used every 50 cm of height. Thus, heights that differ by only 5 cm already appear in different colours. This visualisation clearly shows the lines along which the small height jumps occur. These figures can be used to visually verify the extracted road sides that are shown in Figs. 6, 8 and 10.

The verification of completeness and correctness of the extraction results was performed by comparison with road sides that were manually outlined in an orthophoto. Fig. 11 shows a part of the analysis of crossing 3. A buffer was taken around the reference road sides and the extraction results were labelled as inside or outside the buffer. The completeness was defined as the length of the extracted lines inside the buffer divided by the length of the reference lines. The correctness was defined as the length of the extracted lines inside the buffer divided by the length of all extracted lines. The resulting completeness and correctness numbers are given in table 1. As the amount of false alarms near real road lines is very low, the width of the buffer can be chosen quite large without running the risk of counting other height jump edges as road sides. A buffer width of 50 cm was used for the evaluation.

Crossing	1	2	3
Completeness	0.86	0.85	0.50
Correctness	0.84	0.89	1.00

Table 1: Correctness and completeness statistics.

Although the procedure for the detection of small height jumps does not explicitly search for two planes at slightly different heights, it was found that only few false alarms were created as evidenced by the high correctness numbers in table 1. Most detected height jumps that did not belong to a road side were caused by low vegetation. These detected height jumps were largely eliminated in the check on the minimum required segment length. It would be very quick to manually select and remove the remaining false detections.

An inspection of the road sides in the terrain showed that all locations with unoccluded small height jumps were detected correctly. The deficiencies in the completeness are therefore only caused by the absence of height jumps at the road side or by occlusion of the road sides by parked cars or trees. The occlusion by trees was usually less severe as the survey was performed in the leaf-off season and the used scanner returned up to four echoes per pulse. Trees did therefore not significantly reduce the density of points on the ground.

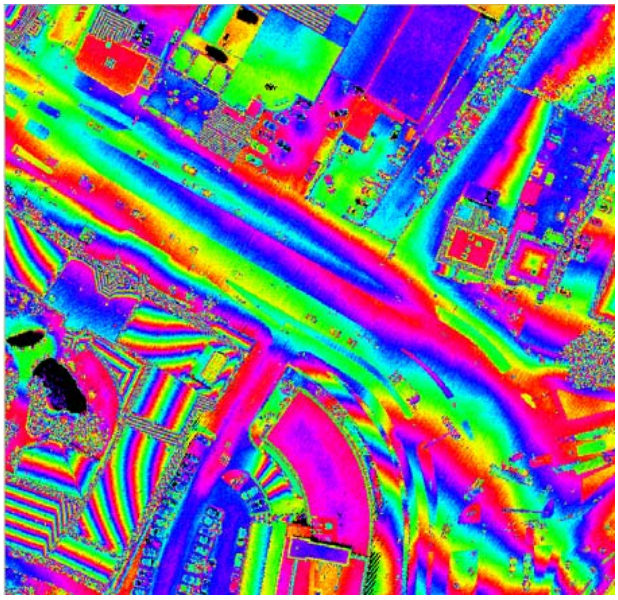

Fig. 5: Colour coded height image of crossing 1 with a colour cycle length of 0.5 m.

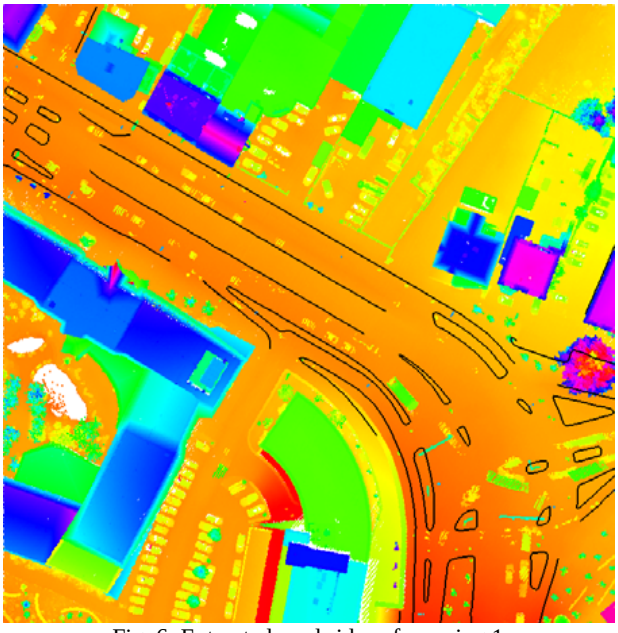

Fig. 6: Extracted road sides of crossing 1.

The results of crossing 1 in Fig. 6 show that the road sides are detected well. The few gaps in the road sides are caused by larger parts without height jumps. Also note that the presence of traffic lights or cars did not disturb the road side extraction.

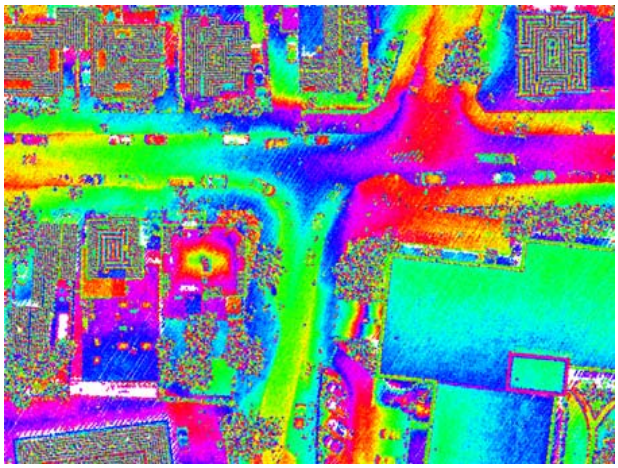

Fig. 7: Colour coded height image of crossing 2 with a colour cycle length of 0.5 m.

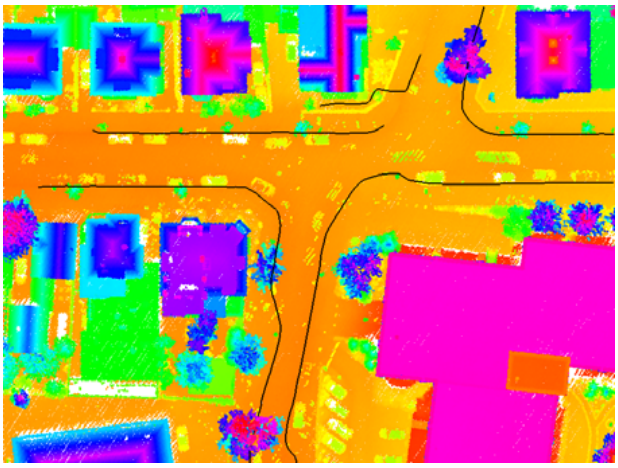

Fig. 8: Extracted road sides of crossing 2.

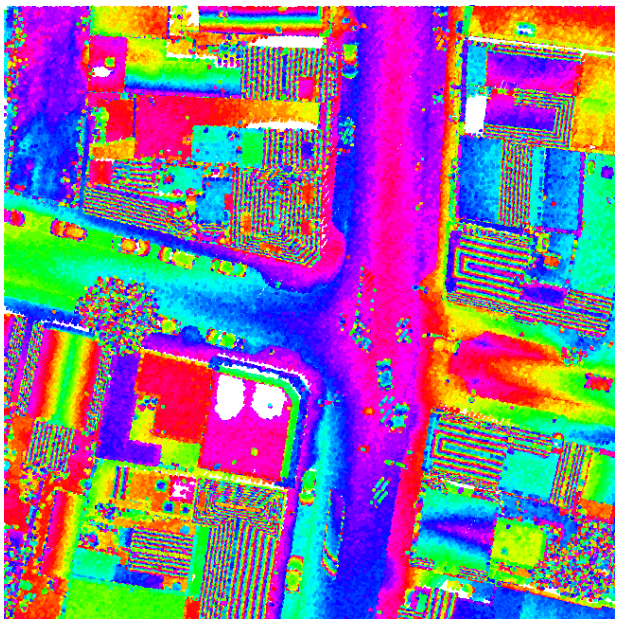

Fig. 9: Colour coded height image of crossing 3 with a colour cycle length of 0.5 m.

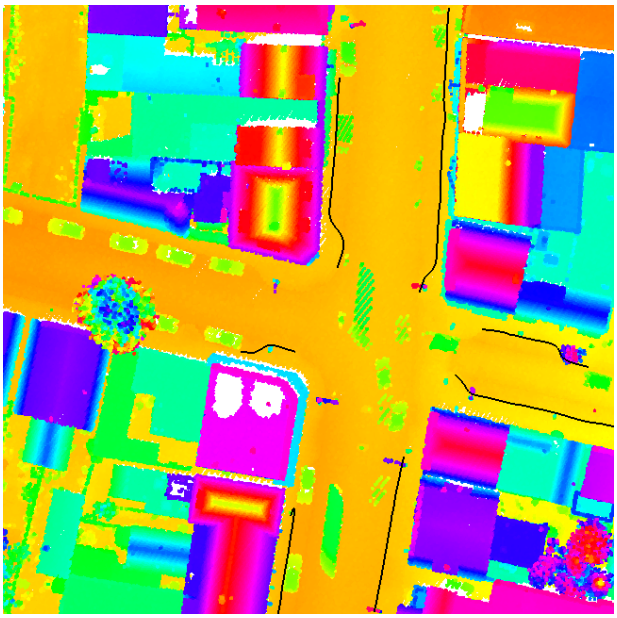

Fig. 10: Extracted road sides of crossing 3.

They also do not lead to false alarms as the height differences are much larger than those of curbstones.

Similar results were obtained for crossing 2. Although several cars are parked next at the road side, the detected pieces of unoccluded road sides could be connected well. In the north part of the crossing, the rules for connecting the segments introduce an erroneous connection between a road segment and a segment in a garden.

Crossing 3 proved to be the most difficult scene. The road side contains several curves for parking lots. The combination of this more complex road side shape, the absent height differences to facilitate crossing with wheelchairs and the occlusion by parked cars only allowed a completeness of 50%. Although a few more road segments were detected than those shown in Fig. 10, connections between these segments could not be made with the formulated rules. As the lengths of the detected segments were below the used threshold of 5 m, these segments were not accepted for the final results of Fig. 10.

Fig. 11: Buffer around road side as manually outlined in an orthophoto (pink) with initially detected road sides (blue) and those accepted after bridging gaps and checking the segment length.

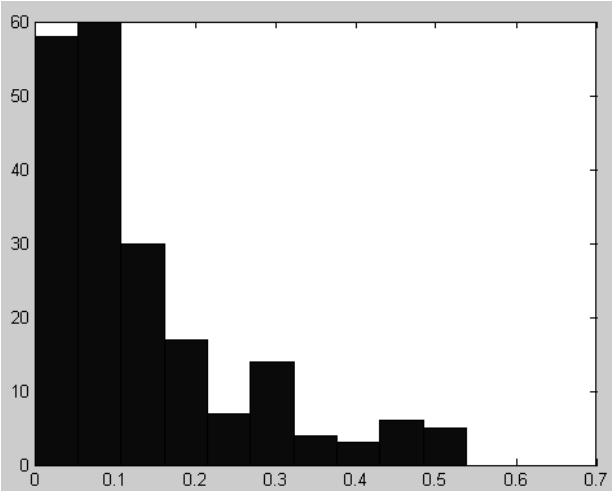

Fig. 12: Frequencies of distances (in m) between the GPS points and the extracted road sides.

The accuracy of the extracted road sides was analysed by a comparison with GPS measurements. Two hundred points on the road sides of crossing 1 were surveyed. The RMS value of the distances between the GPS points and the detected road sides was 0.18 m. The distribution of the differences between the GPS points and the extracted road sides is shown in Fig. 12. The large majority of the differences is smaller than 0.10 m. The largest observed differences are 0.55 m. The systematic offset between the GPS points and the road sides was estimated and found to be 2 cm in X- and 3 cm in Y-direction. These offsets are most likely due to the systematic errors in the airborne laser scanning data. The offsets between overlapping strips had previously been found to be in the same order of magnitude (Vosselman, 2008). Fig. 13 shows a part of the extracted road sides together with the locations of the GPS reference measurements. It shows that the larger errors occur at road side locations with a high curvature. The splines fitted to the extracted point tend to round off the corners. This rounding off is the major source of the errors contributing to the RMS value of 0.18 m. The RMS value computed with only points at road sides with little to no curvature was only 0.08 m.

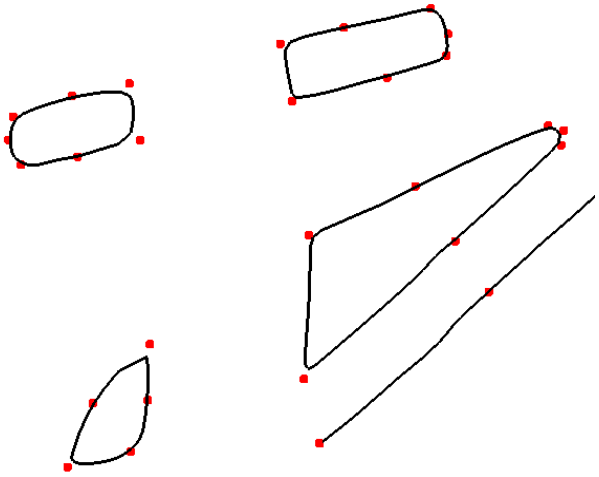

Fig. 13: Extracted road sides with locations of reference data measured with GPS.

Finally, it was also analysed to what extent the point density influences the quality of the road side extraction. The thresholds used in the road side detection were optimised for the densities of 20, 10 and 5 pts/m^2. Table 2 show the results for crossing 1. The correctness of the extracted lines was hardly affected by the reducing the point density. The completeness and accuracy, however, were deteriorating, approximately linear with the average spacing between the laser scanning points.

Point density (pts/m^2)	20	10	5
Completeness	0.86	0.77	0.58
Correctness	0.84	0.84	0.79
RMS (m)	0.18	0.25	0.33

Table 2: Correctness, completeness and accuracy for crossing 1 as a function of the point density.

4. DISCUSSION

The results of this study show that the automated extraction of road sides from airborne laser scanning data is feasible and may be of use in mapping processes if the road sides are bounded by (unoccluded) curbstones. Parked cars occluding the curbstones were found to be the major obstacle in achieving a higher completeness.

The delineation of the road sides could be further improved in various ways. Currently, the algorithm takes the mid points of nearby points on either side of the height jump as a measurement of the jump edge location. If one would only have one point on either side, the midpoint would indeed be the location with the minimum expected error. However, by combining the locations of multiple high and low points along the edge, a more accurate estimate may be made. This problem bears some similarity to the sub-pixel localisation of edges in binary images. A difference, however, is that the data points are not structured in a grid.

Furthermore, a better balance needs to be found between smoothing the detected road sides and following the pattern of the detected height jumps. In line segments with little to no curvature the lines should be further idealised. In contrast, in segments with sharp corners the curve fitting should allow a larger variability in the local curvature.

Finally, the localisation accuracy of the road sides as well as the completion of the detection may be further improved by the integration with imagery. In most laser scanning surveys cameras are used to simultaneously acquire optical imagery. As the spatial resolution of this imagery is usually higher than that of the point cloud, the imagery can be used to obtain more accurate road side outlines. This would lead to a strategy where the point cloud processing is primarily targeting a reliable detection of the road sides and where the image analysis is responsible for the accurate outlining. The image data can also be used to close gaps in the detected road sides that are caused by a local absence of height differences (for carriage drives or wheelchair crossings). In many of these cases the surface material of the pavement next to the road does not change when the pavement is lowered to the road level. Hence, the differences in image colour or texture between the road and pavement surface can be used to find the proper connection between the road side segments detected in the laser scanning data.

REFERENCES

Akel, N. A., Kremeike, K., Filin, S., Sester, M., Doytsher, Y., 2005. Dense DTM generalization aided by roads extracted from LIDAR data. International Archives of the Photogrammetry, Remote Sensing and Spatial Information Science, vol. 36, part 3/W19, Enschede, the Netherlands, pp.54-59.

Brenner, C., 2005. Building reconstruction from images and laser scanning. International Journal of Applied Earth Observation and Geoinformation 6 (3-4), 187-198.

Clode, S.P., Kootsookos, P.J., Rottensteiner, F., 2004a. Accurate Building Outlines from ALS Data. Proceedings 12th Australasian Remote Sensing and Photogrammetry Conference, October 18-22, Fremantle, Perth, Western Australia. http://eprint.uq.edu.au/archive/00001316/01/clode_etal_perth.pdf (accessed March 25, 2009).

Clode, S., Kootsookos, P., Rottensteiner, F., 2004b. The automatic extraction of roads from LIDAR data. International Archives of the Photogrammetry, Remote Sensing and Spatial Information Science, vol. 35, part B3, Istanbul, Turkey, pp. 231-237.

Clode, S., Rottensteiner, F., Kootsookos, P., 2005. Improving city model determination by using road detection from lidar data. International Archives of Photogrammetry, Remote Sensing and Spatial Information Sciences, vol. 36, part 3/W24, Vienna, Austria, pp. 159-164.

de Boor, C., 1978. A Practical Guide to Splines. Springer-Verlag, New York.

Fischler, M., Bolles, R., 1981. Random Sample Consensus: A paradigm for model fitting with applications to image analysis and automated cartography. Communications of the ACM 24 (6), 381-395.

Fugro Aerial Mapping, 2009. FLI-MAP 400. http://www.flimap.nl/download/leaflets/FLIMAP400.pdf (accessed March 25, 2009).

Hatger, C., 2005. On the use of airborne laser scanning data to verify and enrich road network features. International Archives of the Photogrammetry, Remote Sensing and Spatial Information Science, vol. 36, part 3/W19, Enschede, the Netherlands, pp.138-143.

Hatger, C., Brenner, C., 2003. Extraction of Road Geometry Parameters form Laser Scanning and Existing Databases. International Archives of the Photogrammetry, Remote Sensing and Spatial Information Sciences, Dresden, Germany, vol. 34, part 3/W13, pp. 225-230.

Hyyppä, J., Inkinen, M., 1999. Detecting and estimating attributes for single trees using laser scanner. The Photogrammetric Journal of Finland 16 (2), 27-42.

Matikainen, L., Hyyppä, J. Hyyppä, H., 2003. Automatic Detection of Buildings from Laser Scanner Data for Map Updating. In: International Archives of Photogrammetry, Remote Sensing and Spatial Information Sciences, Dresden, Germany, vol. 34, part 3/W13, pp. 218-224.

Persson, Å., Holmgren, J., Söderman, U., 2002. Detecting and measuring individual trees using an airborne laser scanner. Photogrammetric Engineering & Remote Sensing 68 (9), 925-932.

Rieger, W., Kerschner, M., Reiter, T. & Rottensteiner, F. (1999) Roads and buildings from laser scanner data within a forest enterprise. International Archives of Photogrammetry and Remote Sensing, vol. 32, part 3/W14, La Jolla, U.S.A., pp. 185-191.

Rottensteiner, F., 2003. Automatic generation of high-quality building models from LIDAR data. IEEE Computer Graphics & Applications 23 (6), 42-50.

Sampath, A., Shan, J., 2007. Building Boundary Tracing and Regularization from Airborne Lidar Point Clouds. Photogrammetric Engineering & Remote Sensing 73 (7), 805-812.

Vosselman, G., 2008. Analysis of planimetric accuracy of airborne laser scanning surveys. International Archives of Photogrammetry, Remote Sensing and Spatial Information Sciences, vol. 37, part 3A, Beijing, China, July 3-11, pp. 99-104.

Vosselman, G., Kessels, P., Gorte, B.G.H., 2005. The Utilisation of Airborne Laser Scanning for Three-Dimensional Mapping. International Journal of Applied Earth Observation and Geoinformation 6 (3-4), 177-186.

Wang, O., Lodha, S. and Helmbold, D., 2006. A Bayesian Approach to Building Footprint Extraction from Aerial LIDAR Data. Third International Symposium on 3D Data Processing, Visualization and Transmission (3DPVT), Chapel Hill, USA.

Zhou, L., 2009. Extraction of road sides from high point density airborne laser scanning data. M.Sc. thesis, International Institute of Geo-Information Sciences and Earth Observation (ITC), Enschede, the Netherlands, 55 p. http://www.itc.nl/library/papers_2009/msc/gfm/zhou_liang.pdf (Accessed March 27, 2009).